Supporting Information

Synergizing Hydrazine Co-Crystal with Hydrazine Salt of TNAE: A Novel Strategy for Developing Highly Insensitive Explosives

Shreyasi Banik,[a‡] Vikas D. Ghule,[b] and Srinivas Dharavath[a*]

[a]Energetic Materials Laboratory, Department of Chemistry, Indian Institute of Technology Kanpur, Kanpur-208016, Uttar Pradesh, India. orcid.org/ 0000-0003-0511-0607. E-mail: srinivasd@iitk.ac.in

[b]Department of Chemistry, National Institute of Technology Kurukshetra, Kurukshetra-136119, Haryana, India. orcid.org/0000-0002-0967-7777.

Table of Contents

Experimental Procedures

Caution! The compounds in this work are energetic materials that could potentially explode under certain conditions (e.g., impact, friction, or electric discharge). Appropriate safety precautions, such as the use of shields in a fume hood and personal protection equipment (safety glasses, face shields, earplugs, as well as gloves) should be always taken when handling these materials.

General. All reagents were purchased from AKSci or TCI or Merck in analytical grade and were used as supplied. ^{1}H, and ^{13}C{^{1}H} NMR spectra were recorded JEOL DELTA (ECS) 500 (^{1}H, 500 MHz) and ^{13}C{^{1}H} NMR (126 MHz, DMSOd6) nuclear magnetic resonance spectrometer. Chemical shifts for ^{1}H NMR and ^{13}C{^{1}H} NMR spectra are given with respect to external $(CH_3)_4Si$ (^{1}H and ^{13}C). [D6] DMSO was used as a locking solvent unless otherwise stated. IR spectra were recorded using Zn-Se pellets with an ECO-ATR spectrometer (Bruker Alpha II). A single crystal of suitable dimensions was used for data collection. Diffraction intensities were collected on a Bruker APEX-II CCD diffractometer, with graphite monochromated Mo Kα (0.71073 Å) radiation at 100(2) K. Density was determined at room temperature by employing Anton Par Ultra5000 gas pycnometer. Decomposition temperatures (onset) were recorded using a dry nitrogen gas purge and a heating rate of 5 °C min^{-1} on a thermogravimetric differential scanning calorimeter (TGA-DSC (SDT-650)). Impact and friction sensitivity measurements were made using a standard BAM fall hammer and a BAM friction tester.

1,1,2,2-tetranitroaminoethane (1): Compound **1** was prepared according to the literature procedure.[1,2]

Tetrahydaazinium ethane-1,1,2,2-tetrayltetrakis(nitroamide) (2): 1,1,2,2-tetranitroaminoethane (**1**) (0.270 g, 1 mmol) was dissolved in 5 mL of methanol, and to this 80% hydrazine monohydrate (0.3 mL, 4 mmol) was added dropwise at room temperature and the reaction mixture were stirred for 2 hrs at same temperature. The formed brown precipitate was collected by filtration and dried in air to afford desired products **2** in 56% yields (223 mg, 5 mmol). T_d(onset): 120 °C. ^{1}H NMR (500 MHz, DMSO-d6): δ (ppm) 7.30 (s, 2H), 6.57 (s, 20H).^{13}C {^{1}H} NMR (126 MHz, DMSO-d6): δ(ppm) 89.68. IR (ATR, ZnSe, cm^{-1}): 659, 716, 763, 815, 956, 1074, 1228, 1254, 1393, 1524, 1594, 3324. HRMS (ESI-QTOF) m/z: $(M+2H_3O)^+$: Calculated for $C_2H_{22}N_{16}O_8$: 437.2237; Found: 437.2365. Elemental analysis: (%) calculated for $C_2H_{24}N_{16}O_9$: C, 5.77; H, 5.81; N, 53.83. Found: C, 5.76; H, 5.68; N, 53.32.

Synthesis of 4,6-dihydrazineyl-5-nitropyrimidine (3): Compound **1** (270 mg, 1 mmol, 1 eq.) was taken in methanol at 50 ºC (3 ml) and to this excess amount of 80% hydrazine monohydrate (1 mL, 20 mmol) was added. The mixture was stirred at same temperature for 6 hrs and cool down to room temperature. The solvent was evaporated under reduced pressure and isolated yellow coloured solid precipitate in 82% yield (326 mg, 8mmol). The formed precipitate was dissolved in the mixture of solvent methanol/water (1:1 ratio) and left to evaporate slowly at room temperature to obtain suitable crystals. T_d(onset): 185 °C, ^{1}H NMR (500 MHz, DMSO-d6): δ (ppm) 7.30 (s, 2H), 6.54 (s, 28H).^{13}C {^{1}H} NMR (126 MHz, DMSO-d6): δ(ppm) 79.01. HRMS (ESI-QTOF) m/z: $(M+H_3O)^+$: Calculated for $C_2H_{30}N_{20}O_8$: 481.2634; Found: 481.2627.

IR (ATR, ZnSe, cm^{-1}): 662,717, 757, 954, 1171, 1228, 1263, 1360, 1392, 1523, 1593, 3042, 3261, 3317. Elemental analysis: (%) calculated for $C_2H_{30}N_{20}O_8$: C, 5.20; H, 6.58; N, 60.58. Found: C, 5.59; H, 5.43; N, 60.86.

X-Ray crystal structure details

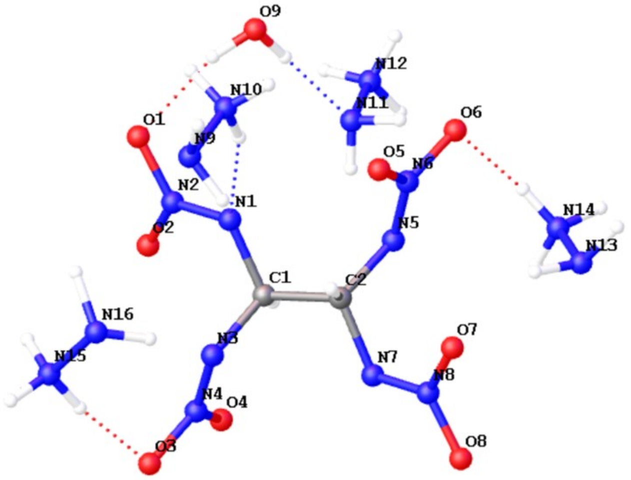

Figure S1: Molecular Structure of **2**.

Table S1: Crystal data and structure refinement for **2**.

CCDC No.	2416101
Empirical formula	$C_2H_{24}N_{16}O_9$
Formula weight	416.37
Temperature/K	100
Crystal system	monoclinic
Space group	$P2_1$
a/Å	9.6301(8)
b/Å	9.1159(9)
c/Å	10.0144(9)
α/°	90
β/°	109.466(2)
γ/°	90
Volume/$Å^3$	828.88(13)
Z	2

ρ_{calc}g/cm^3	1.668
μ/mm^{-1}	0.155
F(000)	440.0
Crystal size/mm^3	0.33 × 0.22 × 0.22
Radiation	MoKα (λ = 0.71073)
2Θ range for data collection/°	4.314 to 56.676
Index ranges	$-12 \le h \le 12$, $-12 \le k \le 12$, $-13 \le l \le 13$
Reflections collected	12490
Independent reflections	4131 [R_{int} = 0.0684, R_{sigma} = 0.0604]
Data/restraints/parameters	4131/1/276
Goodness-of-fit on F^2	1.051
Final R indexes [I>=2σ (I)]	R_1 = 0.0426, wR_2 = 0.1117
Final R indexes [all data]	R_1 = 0.0470, wR_2 = 0.1165
Largest diff. peak/hole / e Å^{-3}	0.72/-0.36
Flack parameter	0.0(7)

Table S2: Fractional Atomic Coordinates (×10^4) and Equivalent Isotropic Displacement Parameters (Å^2×10^3) for **2**. U_{eq} is defined as 1/3 of of the trace of the orthogonalised U_{IJ} tensor.

Atom	***x***	***y***	***z***	**U(eq)**
O4	2868(2)	1409(2)	1929.7(19)	11.1(4)
O6	4148.0(19)	7938(2)	5206.5(19)	11.3(4)
O5	2364(2)	8067(2)	3143.1(19)	10.8(4)
O8	-239(2)	3524(2)	4529(2)	13.0(4)
O1	5182(2)	6017(2)	398.3(19)	10.6(4)
O2	4918(2)	3729(2)	943(2)	14.8(4)
O3	1003(2)	1506(2)	-77(2)	12.9(4)
O7	112(2)	5810(2)	4040(2)	14.0(4)

Table S2: Fractional Atomic Coordinates ($\times 10^4$) and Equivalent Isotropic Displacement Parameters ($Å^2 \times 10^3$) for **2**. U_{eq} is defined as 1/3 of of the trace of the orthogonalised U_{IJ} tensor.

Atom	*x*	*y*	*z*	**U(eq)**
O9	6316(2)	8060(2)	2478(2)	16.4(4)
N2	4561(2)	5063(3)	963(2)	8.5(4)
N7	1420(2)	3975(3)	3520(2)	8.6(4)
N4	1960(2)	2184(3)	973(2)	8.0(4)
N5	3210(2)	5871(3)	4178(2)	8.6(4)
N6	3204(2)	7276(3)	4134(2)	8.3(5)
N12	8055(2)	5978(3)	5608(2)	9.8(4)
N3	1880(2)	3584(3)	940(2)	8.3(4)
N10	2945(2)	8579(3)	545(2)	11.0(4)
N8	436(2)	4454(3)	4016(2)	8.6(5)
N14	4030(2)	6097(3)	7361(2)	12.1(5)
N15	802(3)	3398(3)	-2325(2)	12.9(5)
N1	3605(2)	5532(3)	1509(2)	8.9(4)
N9	1554(3)	8342(3)	-576(3)	17.7(5)
N13	2490(3)	6475(3)	7093(3)	17.3(5)
N11	6546(2)	6098(3)	4681(3)	13.4(5)
N16	351(3)	4846(3)	-1969(2)	15.2(5)
C1	2966(3)	4358(3)	2111(3)	7.3(5)
C2	2135(3)	5141(3)	2979(3)	7.5(5)

Table S3: Anisotropic Displacement Parameters ($Å^2 \times 10^3$) for **2**. The Anisotropic displacement factor exponent takes the form: $-2\pi^2[h^2a^{*2}U_{11}+2hka^*b^*U_{12}+\ldots]$.

Atom	$\mathbf{U_{11}}$	$\mathbf{U_{22}}$	$\mathbf{U_{33}}$	$\mathbf{U_{23}}$	$\mathbf{U_{13}}$	$\mathbf{U_{12}}$
O4	11.8(8)	8.9(10)	10.2(8)	2.3(8)	0.6(7)	2.3(7)
O6	12.8(8)	10.0(9)	7.9(8)	-5.5(8)	-1.1(6)	-4.6(8)

Table S3: Anisotropic Displacement Parameters (Å^2×10^3) for **2**. The Anisotropic displacement factor exponent takes the form: $-2\pi^2[h^2a^{*2}U_{11}+2hka^*b^*U_{12}+\ldots]$.

Atom	**U_{11}**	**U_{22}**	**U_{33}**	**U_{23}**	**U_{13}**	**U_{12}**
O5	15.1(8)	6.4(9)	8.7(8)	1.7(8)	0.9(6)	1.4(8)
O8	13.7(9)	13.1(10)	13.5(9)	0.6(9)	6.4(7)	-4.0(8)
O1	14.1(9)	9.7(9)	9.5(8)	1.1(8)	5.7(7)	-4.9(7)
O2	20.1(10)	7.6(10)	20.1(10)	0.2(8)	11.4(8)	3.2(8)
O3	14.2(9)	10.5(9)	10.8(8)	-3.5(8)	-0.3(7)	-4.6(8)
O7	19.2(10)	6.3(10)	20.3(10)	-0.2(8)	11.6(8)	2.5(8)
O9	23.9(10)	9.9(9)	14.7(9)	0.8(8)	5.5(7)	-1.4(8)
N2	8.8(10)	9.3(11)	7.2(10)	-0.5(8)	2.5(7)	-0.3(8)
N7	9.4(10)	7.4(11)	9.6(9)	-0.1(8)	4.1(8)	-1.8(8)
N4	9.3(9)	7.2(11)	7.3(10)	-0.6(8)	2.3(8)	-1.1(8)
N5	10.6(10)	6.4(11)	8.5(10)	-1.5(8)	2.6(8)	-1.0(8)
N6	7.6(9)	8.8(11)	7.9(10)	-1.8(8)	1.8(8)	-0.6(8)
N12	9.6(9)	9.4(10)	9.7(9)	0.8(9)	2.3(8)	2.6(8)
N3	9.5(10)	6.3(11)	8.3(9)	-1.7(8)	1.6(8)	-0.2(8)
N10	10.4(10)	10.9(11)	11.4(10)	-0.8(9)	3.3(8)	-0.3(9)
N8	9.6(10)	7.8(11)	6.5(9)	-0.8(8)	0.0(8)	-1.8(8)
N14	11.6(10)	12.3(12)	10.5(10)	-0.9(9)	1.3(8)	-2.0(9)
N15	12.5(10)	12.1(13)	11.6(10)	0.7(9)	0.7(8)	1.2(8)
N1	9.7(10)	7.3(11)	9.8(10)	0.0(8)	3.6(8)	0.1(8)
N9	10.4(10)	14.9(14)	22.3(12)	-3.1(10)	-1.7(9)	0.5(9)
N13	14.4(11)	18.7(12)	18.5(11)	1.3(10)	5.2(9)	3.0(9)
N11	7.7(10)	11.7(12)	16.9(11)	1.5(10)	-0.9(8)	-0.7(9)
N16	16.5(11)	13.6(11)	15.3(11)	-0.9(9)	4.9(9)	1.5(9)
C1	7.8(11)	7.0(12)	6.2(11)	-1.2(9)	1.0(9)	-0.9(9)

Table S3: Anisotropic Displacement Parameters ($Å^2 \times 10^3$) for **2**. The Anisotropic displacement factor exponent takes the form: $-2\pi^2[h^2a^{*2}U_{11}+2hka^*b^*U_{12}+\ldots]$.

Atom	**U_{11}**	**U_{22}**	**U_{33}**	**U_{23}**	**U_{13}**	**U_{12}**
C2	8.7(11)	5.7(12)	7.2(11)	1.5(9)	1.2(9)	-0.2(9)

Table S4: Bond Lengths for **2**.

Atom	**Atom**	**Length/Å**	**Atom**	**Atom**	**Length/Å**
O4	N4	1.274(3)	N4	N3	1.278(3)
O6	N6	1.302(3)	N5	N6	1.281(3)
O5	N6	1.274(3)	N5	C2	1.459(3)
O8	N8	1.275(3)	N12	N11	1.445(3)
O1	N2	1.289(3)	N3	C1	1.466(3)
O2	N2	1.265(3)	N10	N9	1.449(3)
O3	N4	1.301(3)	N14	N13	1.458(3)
O7	N8	1.277(3)	N15	N16	1.471(3)
N2	N1	1.290(3)	N1	C1	1.461(3)
N7	N8	1.283(3)	C1	C2	1.539(3)
N7	C2	1.465(3)			

Table S5: Bond Angles for **2**.

Atom	**Atom**	**Atom**	**Angle/°**	**Atom**	**Atom**	**Atom**	**Angle/°**
O1	N2	N1	117.6(2)	N4	N3	C1	116.1(2)
O2	N2	O1	118.3(2)	O8	N8	O7	118.3(2)
O2	N2	N1	124.1(2)	O8	N8	N7	118.1(2)
N8	N7	C2	113.3(2)	O7	N8	N7	123.6(2)
O4	N4	O3	117.9(2)	N2	N1	C1	113.0(2)
O4	N4	N3	126.4(2)	N3	C1	C2	107.97(19)

Table S5: Bond Angles for **2**.

Atom	**Atom**	**Atom**	**Angle/°**	**Atom**	**Atom**	**Atom**	**Angle/°**
N3	N4	O3	115.7(2)	N1	C1	N3	108.0(2)
N6	N5	C2	115.7(2)	N1	C1	C2	105.30(18)
O5	N6	O6	117.9(2)	N7	C2	C1	105.65(19)
O5	N6	N5	125.9(2)	N5	C2	N7	108.6(2)
N5	N6	O6	116.2(2)	N5	C2	C1	108.45(18)

Table S6: Torsion Angles for **2**.

A	**B**	**C**	**D**	**Angle/°**	**A**	**B**	**C**	**D**	**Angle/°**
O4	N4	N3	C1	1.3(4)	N3	C1	C2	N7	61.7(2)
O1	N2	N1	C1	179.7(2)	N3	C1	C2	N5	177.9(2)
O2	N2	N1	C1	0.0(3)	N8	N7	C2	N5	77.6(3)
O3	N4	N3	C1	-179.3(2)	N8	N7	C2	C1	-166.23(19)
N2	N1	C1	N3	-76.8(3)	N1	C1	C2	N7	176.8(2)
N2	N1	C1	C2	168.03(19)	N1	C1	C2	N5	-66.9(2)
N4	N3	C1	N1	132.4(2)	C2	N7	N8	O8	-179.2(2)
N4	N3	C1	C2	-114.2(2)	C2	N7	N8	O7	-0.1(3)
N6	N5	C2	N7	-134.9(2)	C2	N5	N6	O6	179.3(2)
N6	N5	C2	C1	110.8(2)	C2	N5	N6	O5	-0.7(4)

Table S7: Hydrogen Atom Coordinates (Å×10^4) and Isotropic Displacement Parameters (Å^2×10^3) for **2**.

Atom	***x***	***y***	***z***	**U(eq)**
H9C	5992.16	7525.96	1717.29	25
H9D	6409.83	7449.38	3169.7	25
H12A	8629.27	5670.94	5101.71	12

Table S7: Hydrogen Atom Coordinates (Å×10^4) and Isotropic Displacement Parameters (Å^2×10^3) for **2**.

Atom	***x***	***y***	***z***	**U(eq)**
H12B	8111.56	5318.44	6306.44	12
H12C	8375.61	6868.87	6000.2	12
H10A	3648.14	8817.71	160.71	13
H10B	3214.1	7745.08	1067.42	13
H10C	2846.3	9323.39	1112.68	13
H14A	4382.98	6622.39	6771.61	15
H14B	4103.99	5121.71	7203.62	15
H14C	4563.33	6310.62	8276.69	15
H15A	175.66	3108.47	-3184.71	15
H15B	776.14	2735.62	-1654.24	15
H15C	1733.94	3453.3	-2357.77	15
H9A	1060(40)	7790(50)	-70(40)	21
H13A	2040(40)	6440(50)	6110(40)	21
H13B	2360(40)	7510(50)	7480(40)	21
H11A	6100(40)	6590(50)	5260(40)	16
H11B	6220(40)	5220(50)	4730(40)	16
H16A	450(40)	4790(50)	-970(40)	18
H16B	1160(40)	5580(40)	-2170(40)	18
H1	3737.35	3677.81	2710.45	9
H2	1396.53	5852.73	2382.86	9
H9B	1180(40)	9350(40)	-780(30)	9(8)

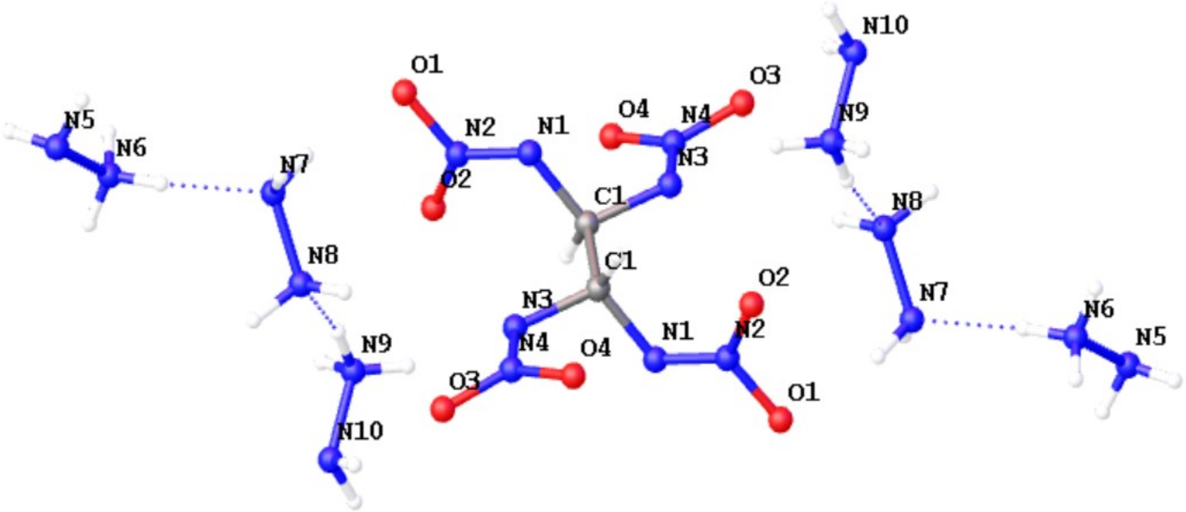

Figure S2: Molecular Structure of **3**.

Table S8: Crystal data and structure refinement for **3**.

CCDC No.	2416100
Empirical formula	$CH_{15}N_{10}O_4$
Formula weight	231.23
Temperature/K	100
Crystal system	monoclinic
Space group	$P2_1/n$
a/Å	10.1038(10)
b/Å	9.4721(9)
c/Å	10.9619(11)
α/°	90
β/°	116.549(3)
γ/°	90
Volume/Å^3	938.47(16)
Z	4
ρ_{calc}g/cm^3	1.637
μ/mm^{-1}	0.148
F(000)	492.0
Crystal size/mm^3	0.33 × 0.22 × 0.22
Radiation	MoKα (λ = 0.71073)
2Θ range for data collection/°	5.98 to 56.652
Index ranges	$-13 \leq h \leq 13$, $-12 \leq k \leq 12$, $-14 \leq l \leq 14$
Reflections collected	13324
Independent reflections	2345 [R_{int} = 0.0602, R_{sigma} = 0.0395]
Data/restraints/parameters	2345/0/196
Goodness-of-fit on F^2	1.049
Final R indexes [I>=2σ (I)]	R_1 = 0.0467, wR_2 = 0.1071
Final R indexes [all data]	R_1 = 0.0559, wR_2 = 0.1137
Largest diff. peak/hole / e Å^{-3}	0.56/-0.33

Table S9: Fractional Atomic Coordinates ($\times 10^4$) and Equivalent Isotropic Displacement Parameters ($Å^2 \times 10^3$) for **3**. U_{eq} is defined as 1/3 of of the trace of the orthogonalised U_{IJ} tensor.

Atom	***x***	***y***	***z***	**U(eq)**
O4	3108.5(13)	3293.2(12)	2811.0(12)	11.0(3)
O3	5362.0(13)	3171.9(12)	4506.6(12)	13.1(3)
O2	6630.0(14)	-1294.1(14)	2459.7(13)	16.7(3)
O1	6727.6(14)	898.0(13)	3157.9(13)	15.5(3)
N2	6323.5(15)	-383.2(15)	3161.2(14)	11.0(3)
N4	4224.0(15)	2527.1(15)	3664.1(14)	10.3(3)
N9	1469.5(16)	7469.2(17)	4501.8(16)	13.1(3)
N1	5590.7(16)	-804.3(15)	3804.0(15)	12.1(3)
N3	4033.5(15)	1188.2(15)	3532.9(15)	11.5(3)
N10	-33.2(16)	7915.4(17)	4162.2(16)	14.5(3)
N5	5681.4(16)	3977.8(16)	7098.4(15)	11.9(3)
N8	1583.4(17)	4546.2(16)	4523.8(16)	15.3(3)
N7	2640.1(16)	4070.8(17)	5860.1(16)	15.3(3)
N6	5823.4(18)	4038.1(17)	8473.8(16)	15.8(3)
C1	5265.5(18)	351.5(17)	4518.7(17)	11.1(3)

Table S10: Anisotropic Displacement Parameters ($Å^2 \times 10^3$) for **3.** The Anisotropic displacement factor exponent takes the form: $-2\pi^2[h^2a^{*2}U_{11}+2hka^*b^*U_{12}+\ldots]$.

Atom	**U_{11}**	**U_{22}**	**U_{33}**	**U_{23}**	**U_{13}**	**U_{12}**
O4	7.6(5)	11.3(5)	12.6(6)	4.1(4)	3.0(4)	3.8(4)
O3	8.5(6)	12.0(6)	14.8(6)	-2.0(5)	1.6(5)	-2.9(4)
O2	17.3(6)	17.5(6)	17.4(6)	-1.4(5)	9.7(5)	4.7(5)
O1	16.6(6)	15.2(6)	14.5(6)	0.0(5)	6.9(5)	-4.9(5)
N2	7.0(6)	13.3(7)	11.2(6)	2.3(5)	2.8(5)	1.8(5)
N4	7.2(6)	11.1(6)	11.5(6)	1.6(5)	3.1(5)	0.2(5)
N9	10.3(7)	16.1(7)	12.7(7)	-1.4(6)	4.9(6)	-2.4(5)
N1	10.4(7)	12.3(6)	15.0(7)	0.7(5)	6.9(5)	0.5(5)
N3	8.8(6)	11.0(6)	13.7(7)	1.6(5)	4.2(5)	0.4(5)
N10	8.7(7)	17.3(8)	17.4(7)	-1.1(6)	5.7(6)	-1.1(5)
N5	9.8(7)	12.7(7)	13.2(7)	0.3(5)	5.1(6)	0.6(5)
N8	10.7(7)	18.7(7)	13.6(7)	0.6(6)	2.8(6)	-0.4(6)
N7	10.6(7)	17.6(7)	15.8(7)	2.7(6)	4.3(6)	0.3(5)
N6	17.5(8)	17.2(7)	14.2(7)	2.3(6)	8.4(6)	1.6(6)
C1	7.9(7)	11.5(7)	12.2(7)	0.7(6)	2.9(6)	0.4(6)

Table S11: Bond Lengths for **3**.

Atom	**Atom**	**Length/Å**	**Atom**	**Atom**	**Length/Å**
O4	N4	1.3150(17)	N9	N10	1.455(2)
O3	N4	1.2644(18)	N1	C1	1.466(2)

Table S11: Bond Lengths for **3**.

Atom	Atom	Length/Å	Atom	Atom	Length/Å
O2	N2	1.2823(19)	N3	C1	1.464(2)
O1	N2	1.2809(19)	N5	N6	1.450(2)
N2	N1	1.292(2)	N8	N7	1.446(2)
N4	N3	1.281(2)	C1	C1[1]	1.533(3)

[1] 1-X,-Y,1-Z

Table S12: Bond Angles for **3**.

Atom	Atom	Atom	Angle/°	Atom	Atom	Atom	Angle/°
O2	N2	N1	118.04(14)	N2	N1	C1	112.37(13)
O1	N2	O2	118.23(14)	N4	N3	C1	114.68(13)
O1	N2	N1	123.70(14)	N1	C1	C1[1]	105.92(16)
O3	N4	O4	117.61(13)	N3	C1	N1	109.24(13)
O3	N4	N3	127.02(14)	N3	C1	C1[1]	107.43(16)
N3	N4	O4	115.37(13)				

[1] 1-X,-Y,1-Z

Table S13: Torsion Angles for **3**.

A	B	C	D	Angle/°	A	B	C	D	Angle/°
O4	N4	N3	C1	-178.10(13)	N2	N1	C1	N3	77.46(16)
O3	N4	N3	C1	2.7(2)	N2	N1	C1	C1[1]	-167.11(15)
O2	N2	N1	C1	-177.73(13)	N4	N3	C1	N1	-134.67(14)
O1	N2	N1	C1	0.4(2)	N4	N3	C1	C1[1]	110.87(18)

[1] 1-X,-Y,1-Z

Table S14: Hydrogen Atom Coordinates (Å×10^4) and Isotropic Displacement Parameters (Å^2×10^3) for **3.**

Atom	*x*	*y*	*z*	U(eq)
H1	6130(20)	910(20)	5040(20)	10(5)
H10A	-610(20)	7450(20)	3420(20)	11(5)
H9A	1690(20)	7760(20)	3870(20)	14(5)
H10B	-80(30)	8800(30)	3990(30)	22(6)
H9B	2080(30)	7850(30)	5270(30)	24(6)
H9C	1490(30)	6530(30)	4560(30)	28(7)
H6A	5240(30)	3350(30)	8520(20)	20(6)
H5A	4720(30)	4040(20)	6530(30)	22(6)
H5B	6060(30)	3190(30)	6940(20)	18(6)
H6B	6750(30)	3790(30)	9070(30)	29(7)
H5C	6150(30)	4760(20)	7010(20)	16(5)
H8A	710(30)	4130(30)	4270(30)	25(6)
H8B	1930(30)	4260(30)	3920(30)	25(6)
H7A	2440(30)	3180(30)	5920(20)	24(6)
H7B	2450(30)	4660(30)	6480(30)	28(6)

NMR, IR, DSC, and TGA plots

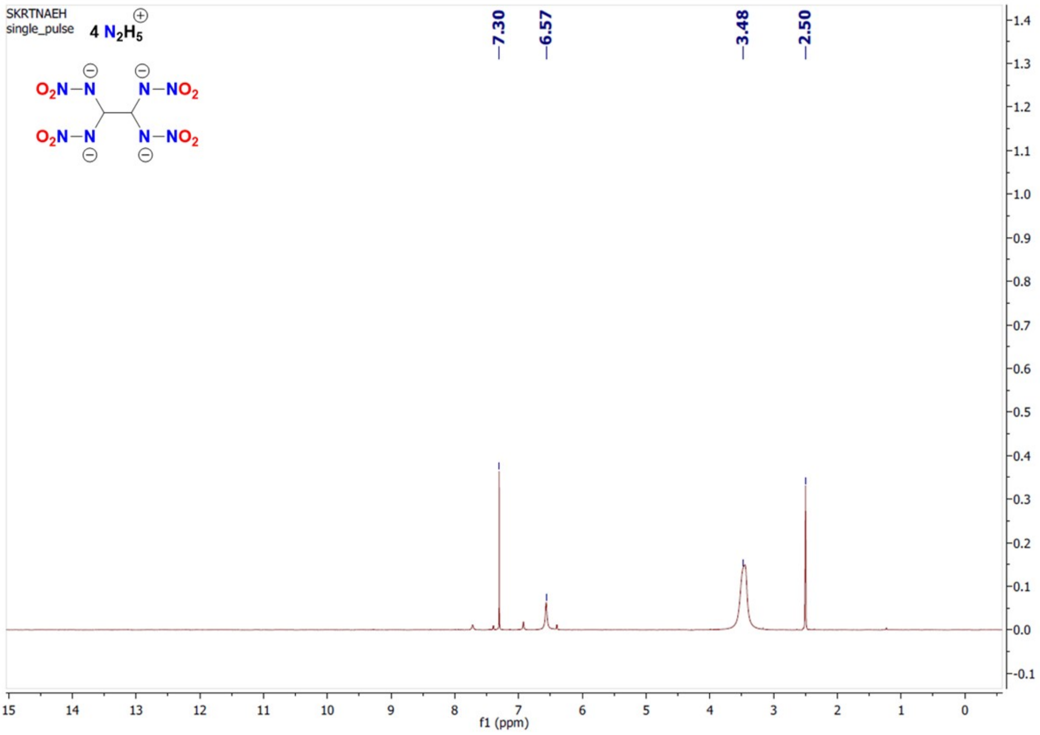

Figure S3: ^{1}H NMR Spectrum of 2.

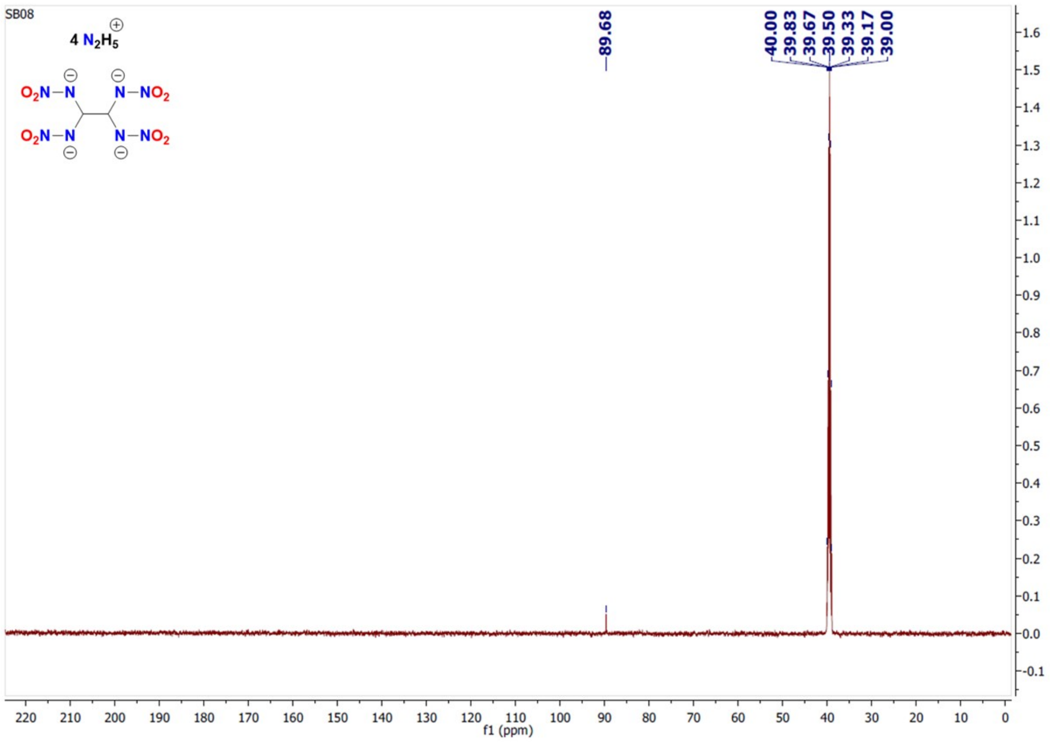

Figure S4: ^{13}C NMR Spectrum of 2.

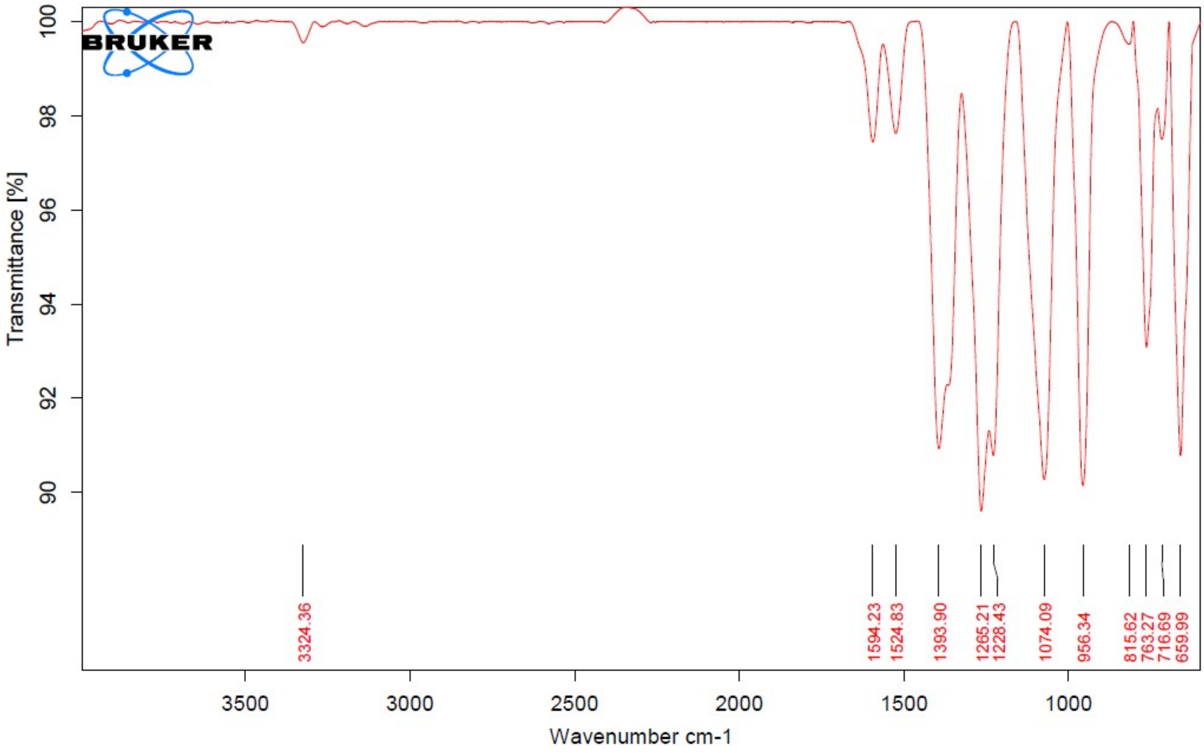

Figure S5: IR Spectrum of Compound 2.

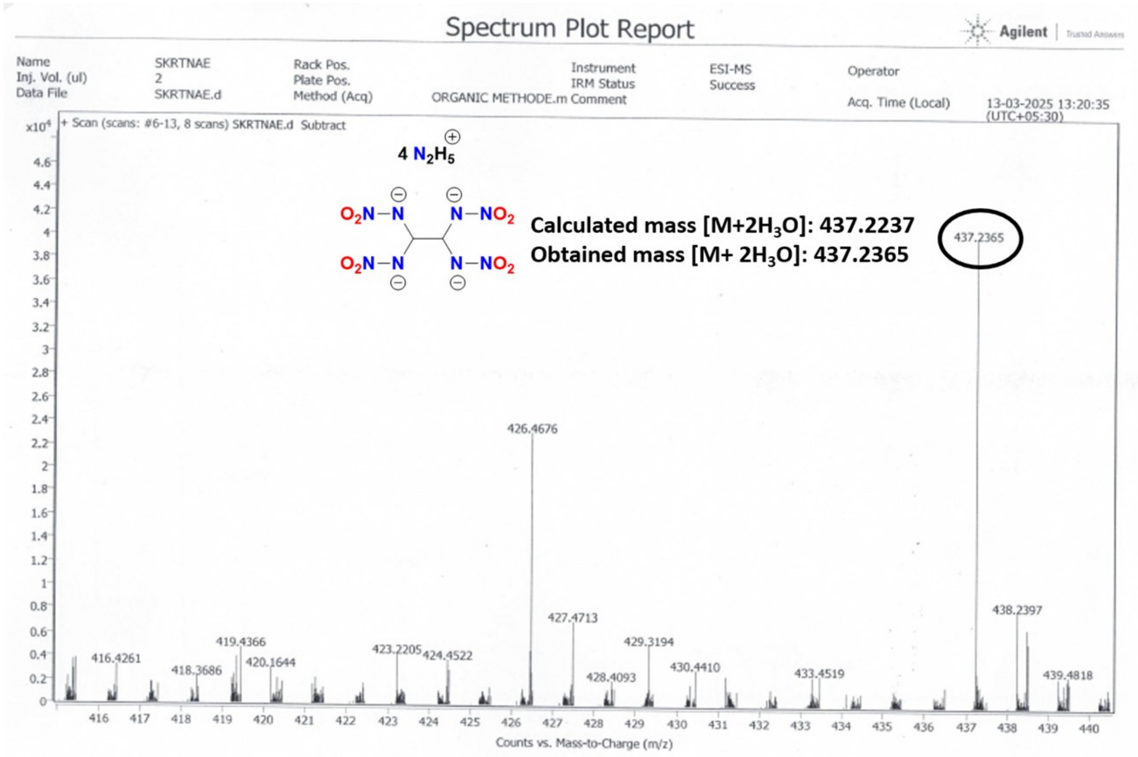

Figure S6: Mass Spectrum of Compound 2.

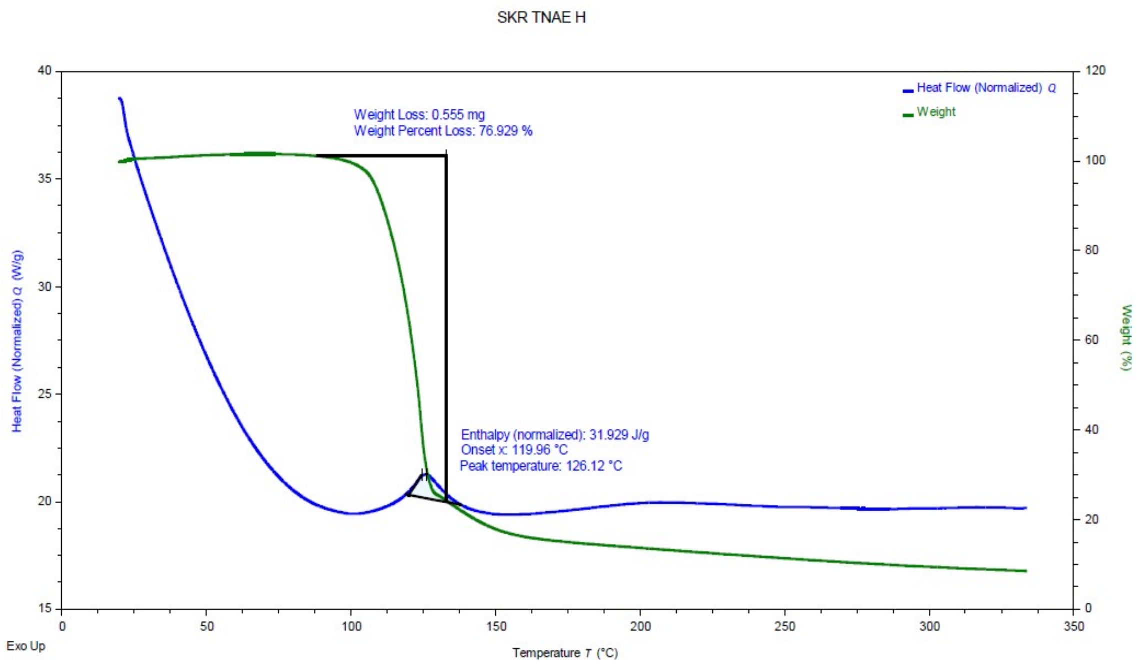

Figure S7: TGA-DSC Plot of Compound 2 at the Heating rate 5 °C min^{-1}.

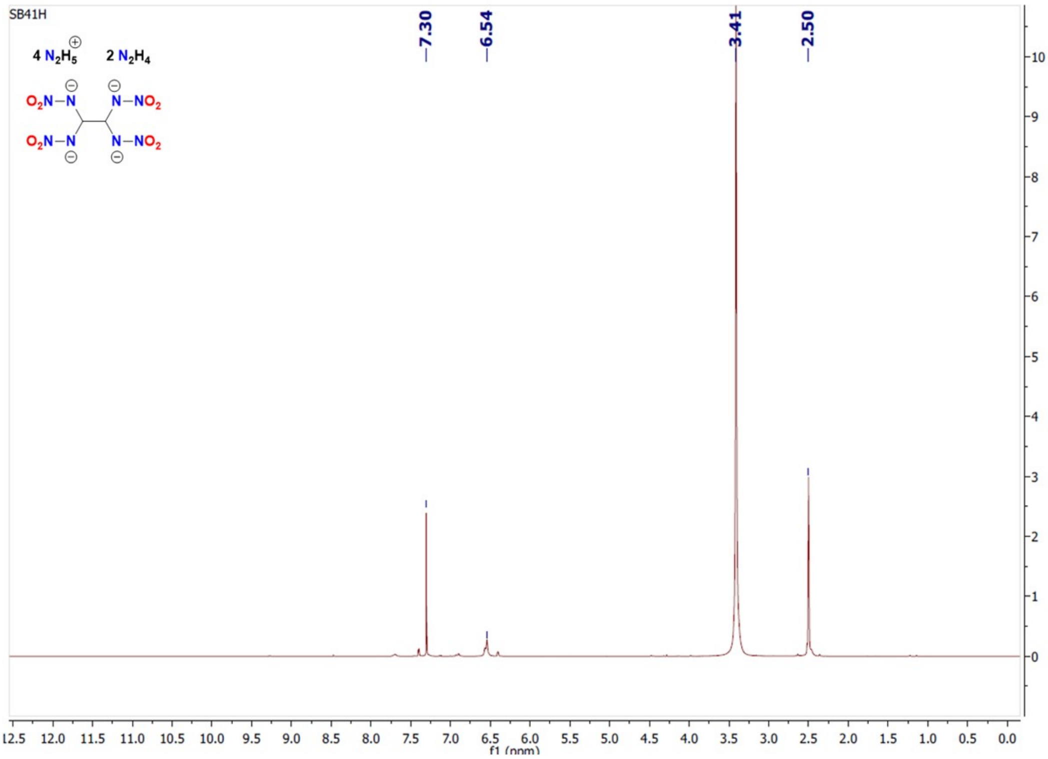

Figure S8: ^{1}H NMR Spectrum of 3.

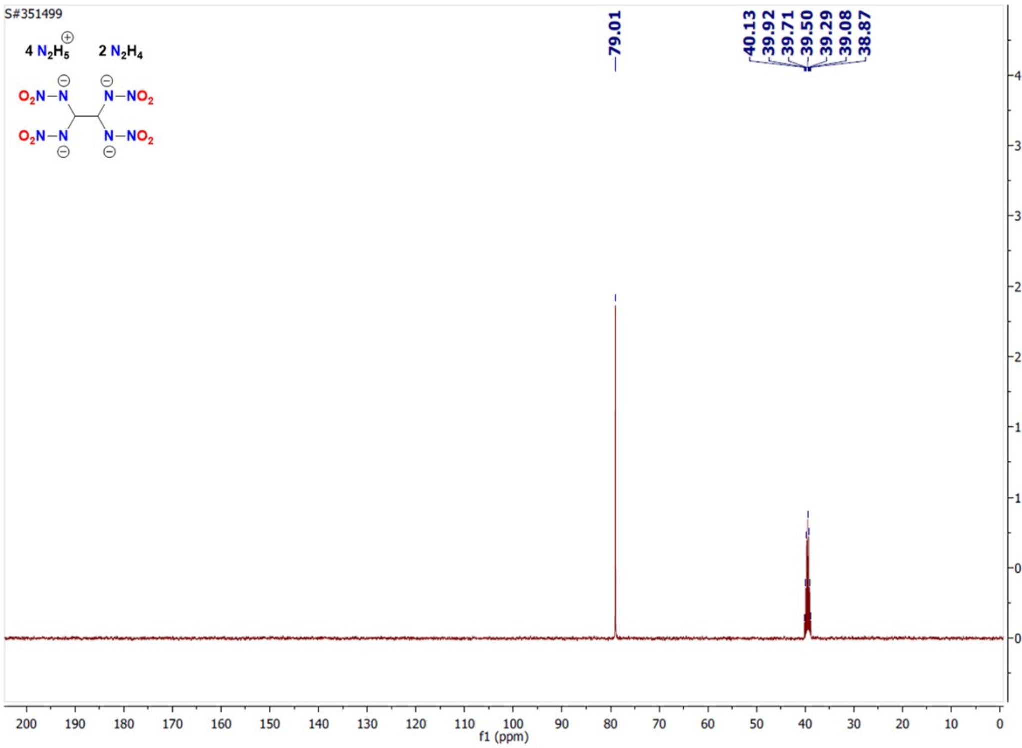

Figure S9: ^{13}C **NMR Spectrum of 3.**

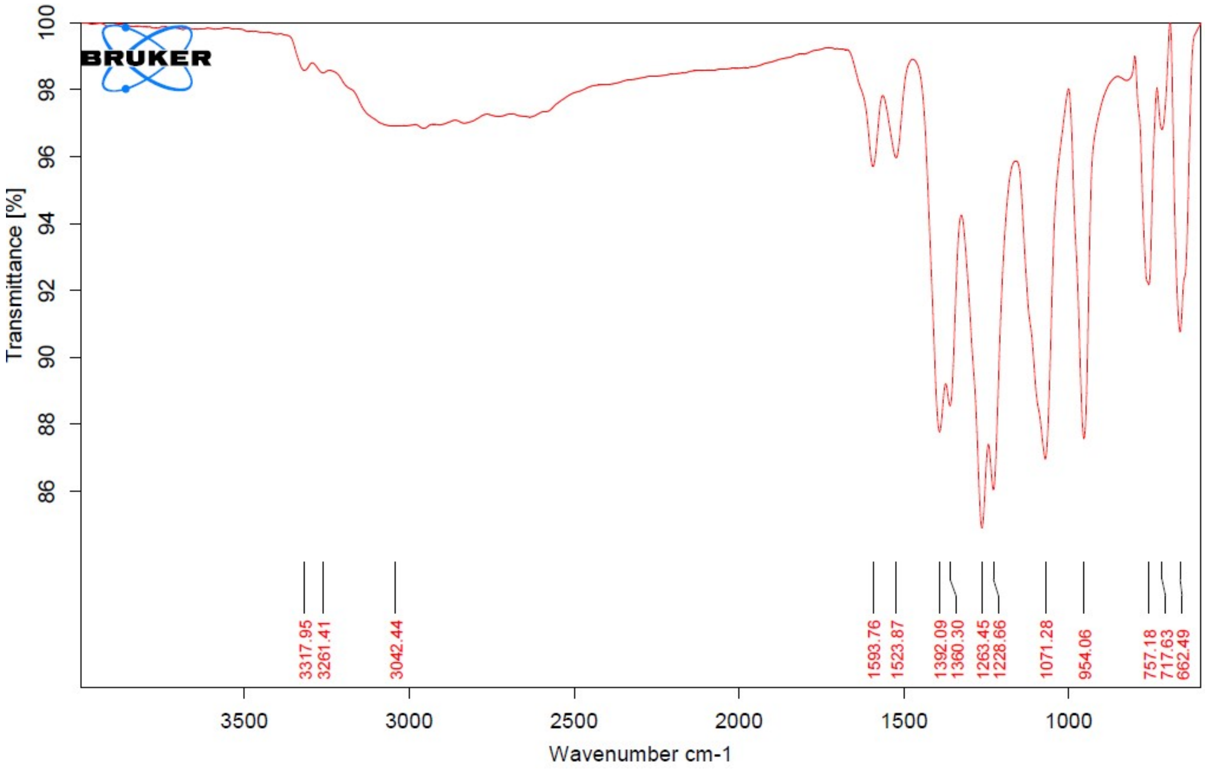

Figure S10: IR Spectrum of Compound 3.

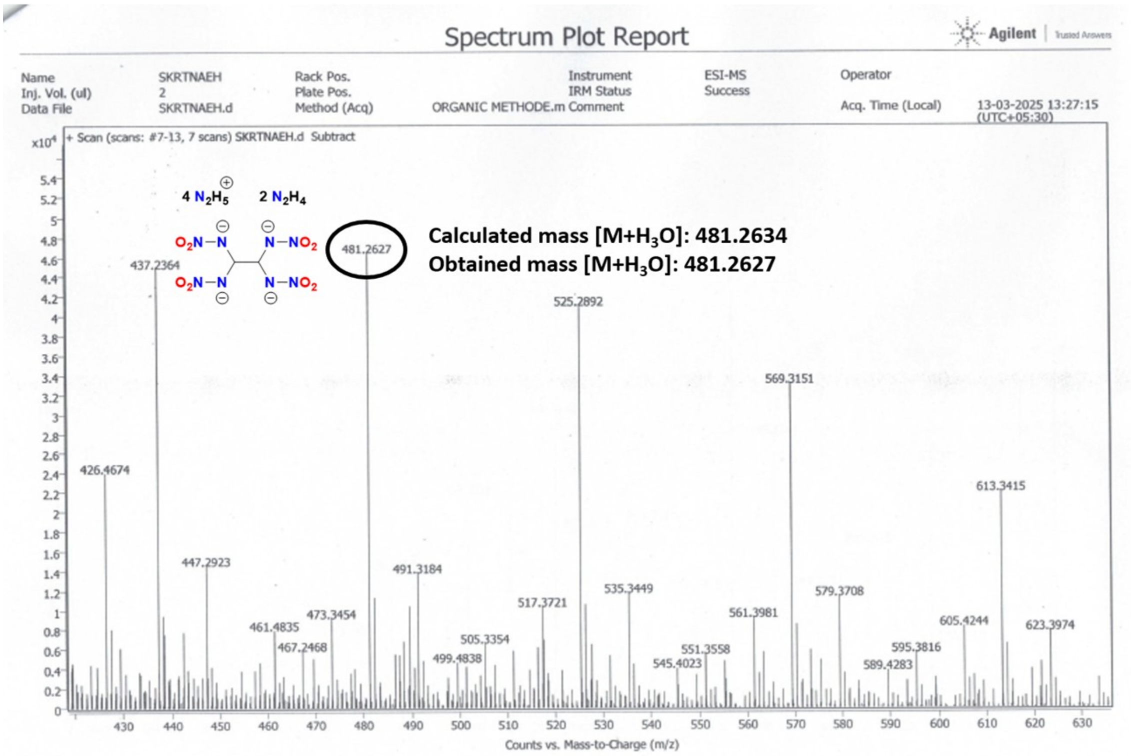

Figure S11: Mass Spectrum of Compound 3.

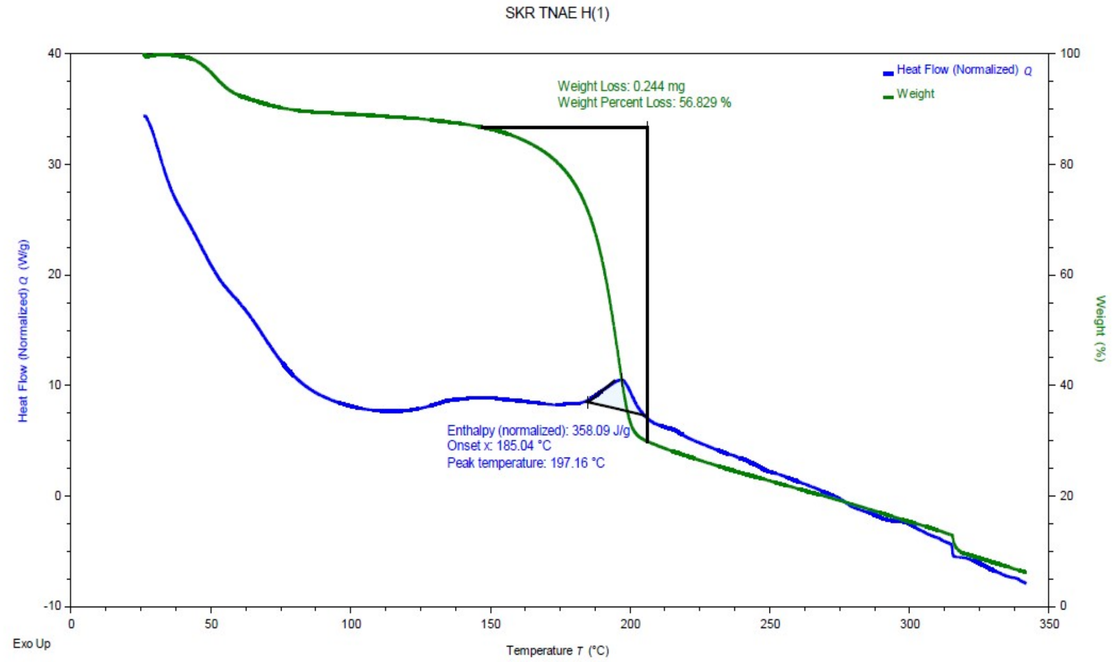

Figure S12: TGA-DSC Plot of Compound 3 at the Heating rate 5 ^{o}C min^{-1}.

Computational Details

Computations were carried out using the Gaussian 09 program suite.[3] The structure optimizations are performed with M06-2X/def2-TZVPP level of theory and characterized to be true local energy minima on the potential energy surface and no imaginary frequencies were found. Heat of formation (HOF) is a measure of energy content of an energetic material that can decompose, ignite and explode by heat or impact. It enters into the calculation of explosive and propellant properties such as detonation velocity, detonation pressure, heat of detonation and specific impulse. However, it is impractical to determine the HOF of novel energetic materials because of their unstable intermediates and unknown combustion mechanism. Gas-phase heats of formation for TNAE neutral compound and its tetra anionic component were calculated using the isodesmic reaction approach (see Figure S13). Calculated total energies and related data for reference compounds and target compounds is listed in Tables S15 and S16.

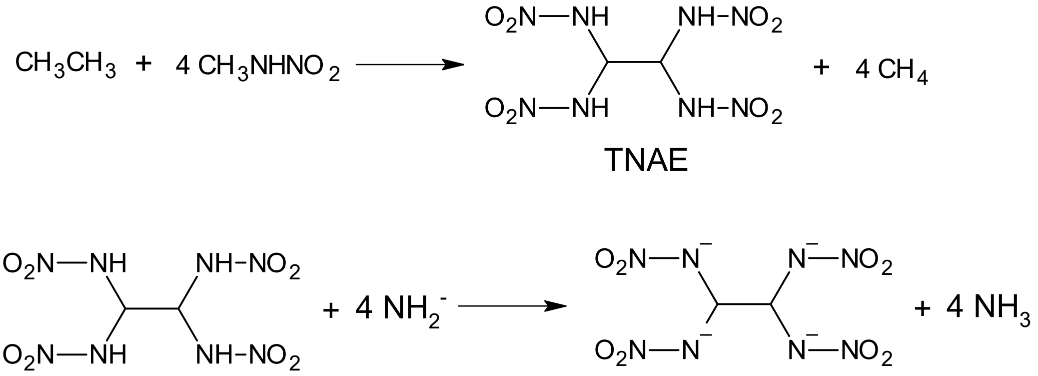

Figure S13: Designed isodesmic reactions for the prediction of gas phase heats of formation TNAE and its anion.

Based on the Born–Haber cycle (shown in Figure S14), the heat of formation of an ionic compound can be simplified by subtracting the lattice energy of the salt (H_L) from the total heat of formation of salt (see Table S17) *i.e.* sum of the heats of formation of the cation and anion as shown in equation (3).

$$\text{HOF (salt, 298 K)} = \text{HOF (cation, 298 K)} + \text{HOF (anion, 298 K)} - H_L \qquad (3)$$

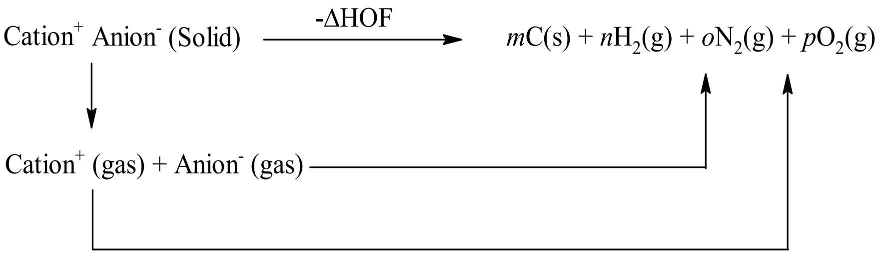

Figure S14: Born-Haber cycle for the formation of energetic salts.

Lattice potential energy is the energy associated with the process in which a crystalline solid lattice, M_pX_q is converted into its constituent gaseous ions, ${}_pM^{q+}$ (g) and ${}_qX^{p-}$ (g). The lattice energy can be predicted with reasonable accuracy by using Jenkins' equation (4).[4]

$$\mathrm{H_L} = U_{\mathrm{POT}} + [p(\frac{n_M}{2} - 2) + q(\frac{n_X}{2} - 2)]RT \tag{4}$$

where *nM* and *nX* depend on the nature of the ions M_p^+ and X_q^-, respectively, and are equal to 3 for monoatomic ions, 5 for linear polyatomic ions, and 6 for nonlinear polyatomic ions. When lattice potential energy (U_{POT}), is incorporated and made part of a Born–Haber cycle, it needs to be converted into a lattice enthalpy term. This lattice enthalpy (H_L) involves correction of the U_{POT} term by an appropriate number of RT terms. The HOF of compound 3 was calculated by adding the HOF of hydrazine molecules and salt 2, and the computed value is -92.08 kJ/mol.

Table S13: Calculated total energies at 298K (E_0), zero-point energies (ZPE), and thermal corrections (H_T) and experimental HOF_{gas} of reference compounds used isodesmic reaction at the M06-2X/def2-TZVPP level.

Compd.	**E_0 (a.u.)**	**ZPE (au)**	**H_T (au)**	**HOF_{gas} (kJ/mol)**
CH_4	-40.453065	0.0449	0.0038	-74.8
CH_3CH_3	-79.727235	0.075	0.0045	-84
NH_3	-56.513648	0.0345	0.0038	-45.94
CH_3NHNO_2	-300.274649	0.0684	0.0060	-3.76[a]
NH_2^-	-55.856335	0.0186	0.0038	111.75[a]

[a] Calculated using G4 method.

Table S14: Calculated total energies (E_0), zero-point energies (ZPE), and thermal corrections (H_T) for TNAE and its anion at the M06-2X/def2-TZVPP level.

Compd.	**E_0 (a.u.)**	**ZPE (au)**	**H_T (au)**	**HOF_{gas}/HOF_{anion} (kJ/mol)**
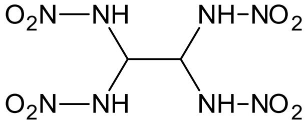	-1119.032178	0.1592	0.0170	151.3
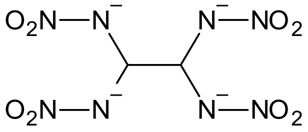	-1116.286576	0.1039	0.0162	1087.5

Table S15: Energy content of salts **2**.

Compd.	**HOF_c[a]**	**HOF_a[b]**	**U_{Pot}[c]**	**H_L[d]**	**HOF_{salt}[e]**
2	769.5	1087.5	4340.54	4352.93	-187.43

[a]Heat of formation of cation (kJ mol^{-1}). HOF_c data for cations is obtained from Ref. 5. [b]Heat of formation of anion (kJ mol^{-1}). [c]Lattice potential energy (kJ mol^{-1}). [d]Lattice energy (kJ mol^{-1}). [e]Heat of formation of salt (kJ mol^{-1}).

Table S16: Optimized coordinates of TNAE at M06-2X/def2TZVPP level of theory.

6	-0.766691000	-0.003915000	-0.055078000
6	0.766674000	0.003910000	0.055064000
7	1.340066000	-1.082355000	-0.746920000
7	1.256079000	1.249346000	-0.455675000
7	-1.340101000	1.082344000	0.746899000
7	-1.256079000	-1.249359000	0.455681000
7	2.423472000	1.737645000	0.095328000
8	3.117277000	0.936761000	0.678692000
8	2.649876000	2.901784000	-0.095780000
7	1.860205000	-2.161115000	-0.066437000
8	1.318901000	-2.447406000	0.985891000
8	2.762128000	-2.748068000	-0.592583000

7	-2.423492000	-1.737655000	-0.095300000
8	-3.117340000	-0.936761000	-0.678594000
8	-2.649880000	-2.901799000	0.095784000
7	-1.860158000	2.161142000	0.066423000
8	-1.318817000	2.447419000	-0.985891000
8	-2.762121000	2.748086000	0.592512000
1	-1.061604000	0.136778000	-1.096651000
1	1.061587000	-0.136796000	1.096637000
1	1.996855000	-0.793432000	-1.461494000
1	0.609923000	1.987553000	-0.722095000
1	-1.996916000	0.793422000	1.461448000
1	-0.609892000	-1.987579000	0.722006000

Table S17: Optimized coordinates of TNAE anion at M06-2X/def2TZVPP level of theory.

6	0.778120000	0.040535000	-0.089263000
6	-0.778089000	-0.040510000	0.089262000
7	-1.426351000	1.000964000	-0.722328000
7	-1.197222000	-1.346258000	-0.448299000
7	1.426366000	-1.000949000	0.722347000
7	1.197271000	1.346273000	0.448293000
7	-2.301181000	-1.803379000	-0.015169000
8	-3.021745000	-1.237547000	0.862905000
8	-2.728361000	-2.920371000	-0.492995000
7	-2.109414000	1.895626000	-0.124342000
8	-2.229899000	2.016413000	1.127458000
8	-2.730512000	2.754092000	-0.858560000
7	2.301212000	1.803409000	0.015140000
8	3.021761000	1.237590000	-0.862967000
8	2.728389000	2.920404000	0.492951000
7	2.109378000	-1.895656000	0.124376000

8	2.229820000	-2.016508000	-1.127423000
8	2.730465000	-2.754121000	0.858615000
1	1.026898000	-0.063698000	-1.144252000
1	-1.026857000	0.063699000	1.144257000

Reference

(1) C. Zhu, Z. Meng, Z. Xu, W. Liu, Y. Liu, X. Shi, Y. Liu, T. Xie, *Cent. Eur. J. Energ. Mater.* **2018**, *15*, 435–444.

(2) M. Born, M. A. C. Härtel, T. M. Klapötke, M. Mallmann, J. Stierstorfer, *Zeitschrift fur Anorg. und Allg. Chemie* **2016**, *642*, 1412–1418.

(3) Gaussian 09, Revision E.01, M. J.Frisch, G. W. Trucks, H. B. Schlegel, G. E. Scuseria, M A. Robb, J. R. Cheeseman, G. Scalmani, V. Barone, B. Mennucci, G. A. Petersson, H. Nakatsuji, M Caricato, X. Li, H. P. Hratchian, A. F. Izmaylov, J. Bloino, G. Zheng, J. L. Sonnenberg, M. Hada, M. Ehara, K. Toyota, R. Fukuda, J. Hasegawa, M. Ishida, T. Nakajima, Y. Honda, O. Kitao, H. Nakai, T. Vreven, Jr. J. A. Montgomery, J. E. Peralta, F. Ogliaro, M. Bearpark, J. J. Heyd, E. Brothers, K. N. Kudin, V. N. Staroverov, R. Kobayashi, J. Normand, K. Raghavachari, A. Rendell, J. C. Burant, S. S. Iyengar, J. Tomasi, M. Cossi, N. Rega, J. M. Millam, M. Klene, J. E. Knox, J. B. Cross, V. Bakken, C. Adamo, J. Jaramillo, R. Gomperts, R. E. Stratmann, O. Yazyev, A. J. Austin, R. Cammi, C. Pomelli, J. W. Ochterski, R. L. Martin, K. Morokuma, V. G. Zakrzewski, G. A. Voth, P. Salvador, J. J. Dannenberg, S. Dapprich, A. D. Daniels, O. Farkas, J. B. Foresman, J. V. Ortiz, J. Cioslowski, D. J. Fox, *Gaussian*, Inc., Wallingford CT, **2013**.

(4) Jenkins, H. D. B.; Tudela, D.; Glasser, L. Lattice Potential Energy Estimation for Complex Ionic Salts from Density Measurements. *Inorg. Chem.* **2002**, 41, 2364-2367.